TIDAL STRESS PATTERNS ON EUROPA'S CRUST*

RICHARD GREENBERG, GREGORY V. HOPPA*,
GWEN BART and TERRY HURFORD
Lunar and Planetary Laboratory, University of Arizona, Tucson, AZ 85721, USA

Abstract. The ice crust of Europa probably floats over a deep liquid-water ocean, and has been continually resurfaced by tectonic and thermal processes driven by tides. Tidal working causes rotational torque, surface stress, internal heating, and orbital evolution. The stress patterns expected on such a crust due to reorientation of the tidal bulge by non-synchronous rotation and due to orbital eccentricity, which introduces periodic ('diurnal') variations in the tide, are shown as global maps. By taking into account the finite rate of crack propagation, global maps are generated of cycloidal features and other distinctive patterns, including the crack shapes characteristic of the wedges region and its antipode on the sub-Jovian hemisphere. Theoretical maps of tidal stress and cracking can be compared with observed tectonics, with the possibility of reconstructing the rotational history of the satellite.

Key words: Europa, stress, tides

1. Introduction

Jupiter's satellite Europa is comparable in size to the Earth's Moon. However, its surface is predominantly composed of water ice, and its density profile indicates that the outer 100–150 km consists of H_2O as well (Anderson et al., 1988). Most of this thick water layer is likely in the liquid state with only a relatively thin shell of ice at the surface. Also unlike the Moon, there are very few impact craters. The current surface is therefore very young (less than $\sim$50 million years old; Zahnle et al., 1998), as a result of continual renewal by several resurfacing processes. These processes likely involve interaction of the surface with the underlying ocean, and all are driven by tides. The observed character of Europa, and the processes that govern it were reviewed at the IAU Colloquium on Astrophysical Tides (Greenberg, 2002, see also Greenberg et al., 2002a, and the references cited therein).

Tides have controlled Europa's physical evolution and resurfacing in several ways. Tidal friction provides the dominant *internal heat* source, keeping the global ocean liquid as well as allowing crustal melt and thickness variability (e.g. O'Brien et al., 2002). Tides generate *rotational torque* that tends to maintain non-synchronous rotation (Greenberg and Weidenschilling, 1984; Greenberg et al., 2002b), especially plausible for Europa given that tidal heating makes it unlikely that there are frozen-in asymmetries capable of locking onto the direction of Jupiter. Over the long term, tidal deformation of the resonantly coupled Galilean

*Prepared for the Proceedings of IAU Colloquium 189, "Astrophysical Tides" in Nanjing, China.

*Present address: Raytheon Missile Systems, Tucson, AZ, USA.

Celestial Mechanics and Dynamical Astronomy **87:** 171–188, 2003.

satellites contributes to *orbital change* (reviewed by Greenberg, 1982, 1989, see also Peale and Lee, 2002), including changes in orbital eccentricities, which modify the amplitudes of diurnal tides. Tides also generate the periodic *global stresses* that crack and displace the surface crust, creating the complex tectonic record visible on Europa's surface.

Evidence for tidally driven tectonics is visible at all scales on Europa. Global crack patterns are marked by dark lines visible even at low resolution. Cracks are often marked by the sets of double ridges that they produce, which cover much of the surface and represent a major component of resurfacing. Dilation along cracks creates new surface as underlying material fills the gaps, and shear along cracks ('strike-slip faults') displaces adjacent plates of crust.

The rough correlation of global-scale lineament patterns with tidal stress patterns was first noted by Helfenstein and Parmentier (1983) on Voyager images. Recognition that Europa could be spinning non-synchronously (Greenberg and Weidenschilling, 1984) led to consideration of the possibility that the observed tectonic patterns might contain some record of such reorientation (Helfenstein and Parmentier, 1985; McEwen, 1986). Such non-synchronous rotation must be very slow relative to the direction of Jupiter (Greenberg et al., 2002b). With the arrival of Galileo images of Europa, more detailed comparisons of observed tectonics with theoretical tidal stress became possible. Geissler et al. (1998a, b) showed how systematic reorientations of crack patterns with age could be explained by passage of a given region through a varying tidal stress field during non-synchronous rotation. Greenberg et al. (1998) refined that theory by including the periodic stress due to orbital evolution (the 'diurnal tide'). They found that cracking seemed to have occurred at maximum diurnal tension, only after a background stress due to non-synchronous rotation had built up enough so that the total stress exceeded the tensile strength of the ice crust.

Understanding of tidal stress patterns led to explanation of other aspects of the tectonic record. The 'strike-slip faults' were shown to correlate with theoretical predictions based on diurnal stress variations (Hoppa et al., 1999a, 2000). That result was exploited to demonstrate that polar wander had occurred (Sarid et al., 2002). Moreover, distinctive and ubiquitous cycloidal-shaped crack patterns, which had been a puzzle since they were first seen in Voyager images, have also been explained by diurnal changes in tidal stress (Hoppa et al., 1999b).

Calculations of tidal stress have been done as needed to investigate the various tectonic phenomena described above. Helfenstein and Parmentier (1983, 1985) displayed global stress orientations, but not magnitudes. Greenberg et al. (1998) introduced global maps that showed principal components of stress on the ice shell as a function of location, which provided both the orientation information as well as the magnitude and character (e.g. predominant compression, tension, or shear) of the stress.

There is a continuing need for complete documentation of the tidal theory as ongoing studies of Europan tectonics become increasingly sophisticated and detailed,

unraveling increasingly complex time sequences going back further in time. Until now, most geologists have had access to theoretical models for only a few selected tidal stress conditions to support their efforts to explain aspects of the tectonic record. For example, Figueredo and Greeley (2000) and Kattenhorn (2002) depended on cases displayed by Greenberg et al. (1998). Here we assemble a much more complete set of global stress maps than has been available before in order to facilitate interpretation of observed tectonics. Then we show an example of our recent applications of these stress fields.

2. Stress due to Non-synchronous Rotation

The tidal figure of Europa deviates from a sphere by a radial displacement given by

$$H = h\left(\frac{M}{m}\right)\left(\frac{R}{a}\right)^3 \frac{R(3\cos^2\theta - 1)}{2} \tag{1}$$

where H is the local height of the tide at the surface, M is Jupiter's mass, m is Europa's mass, R is the radius of Europa, a is the distance from Jupiter, θ is the angular distance along Europa's surface from the sub-Jupiter point, and h is the Love number. For Europa, $(M/m)(R/a)^3R$ is about 800 m. If the satellite were fluid, h would be 2.5, but with rock below the water layer a better estimate is about 1.2 (Yoder and Sjogren, 1996; Moore and Schubert, 2000). Thus the height of the tide (at the sub- or anti-Jovian point relative to the average radius) is about 1 km.

We model the crust as an elastic sheet overlying the tidally deforming body. We assume that this sheet is decoupled from the rest of the body in the sense that there is no shear stress between it and what lies below, a reasonable assumption given the likelihood of a global liquid water ocean. We treat the ice sheet as a two-dimensional sheet, that is, we ignore its thickness and ignore any stress components normal to the surface. We also assume that the ice sheet is continuous and uniform in its elastic properties. In reality continuity is disrupted whenever a crack forms, and real material is unlikely to be uniform on a global scale. However, as a first approximation to understanding global stress fields, these approximations are reasonable.

If Europa were on a circular orbit and rotating synchronously, this tide would be fixed relative to the body, and any elastic stress in the ice crust would relax. However, Europa is actually in an eccentric orbit, driven by the Laplace resonance with Io and Ganymede, and likely rotates non-synchronously, as driven by tidal torques.

We first consider the effect of non-synchronous rotation on stress in the crust. In fact, demonstration of non-synchronous rotation came from interpretation of observed tectonics resulting from tidal stress (Greenberg et al., 2002b). The period of rotation relative to the direction of Jupiter is probably ~50,000 years. Suppose

the crust were in a relaxed state with a tidal bulge, and then the tidal bulge were reoriented relative to the crust by non-synchronous rotation. This could happen if the whole body were rotating non-synchronously or if only the crust rotated non-synchronously. In the process, the crust must distort to accommodate the changing shape and stress accumulates.

We calculate the stress by exploiting the equilibrium solution for an elongated (or flattened) spherical shell (Vening-Meinisz, 1947; Melosh, 1980) in the following way. We note that the reorientation of the tidal bulge is equivalent to first removing the tidal bulge (stressing the crust) and then add back the tidal bulge in the new orientation (stressing it again). The stress in each step is calculated directly from the Vening-Meinisz/Melosh theory and then we add them together. The magnitude of the stress field is proportional to $\mu(1 + \nu)/(5 + \nu)$, where μ is the shear modulus and ν is the Poisson ratio. The plots of stress shown in this paper (Figures 1–3) are based on values of $\mu = 9.3 \times 10^9$ Pa and $\nu = 0.33$ (Turcotte and

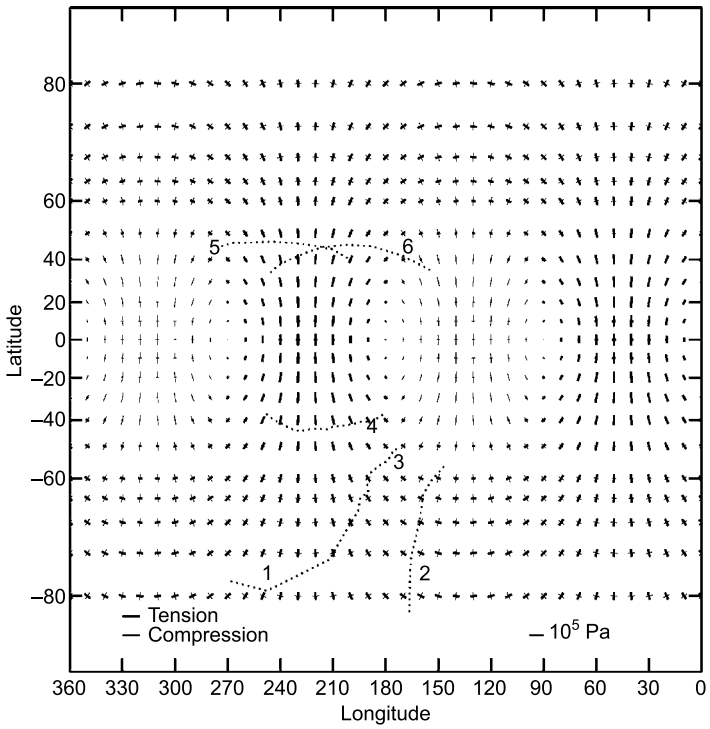

Figure 1. Map of stress induced in a thin elastic shell due to a 1° rotation of a tidal bulge of the magnitude of Europa's primary tidal component. Crossed lines indicate the orientation and magnitude of the principle components, with bold lines indicating compression and fine lines tension. Note scale bar for magnitude of the stress. Locations of several major Europan lineaments are indicated by dotted lines. Several major observed lineaments are shown: (1) Astypalaea Linea; (2) Thynia Linea; (3) Libya Linea; (4) Agenor linea; (5) Cadmus Linea; (6) Minos Linea.

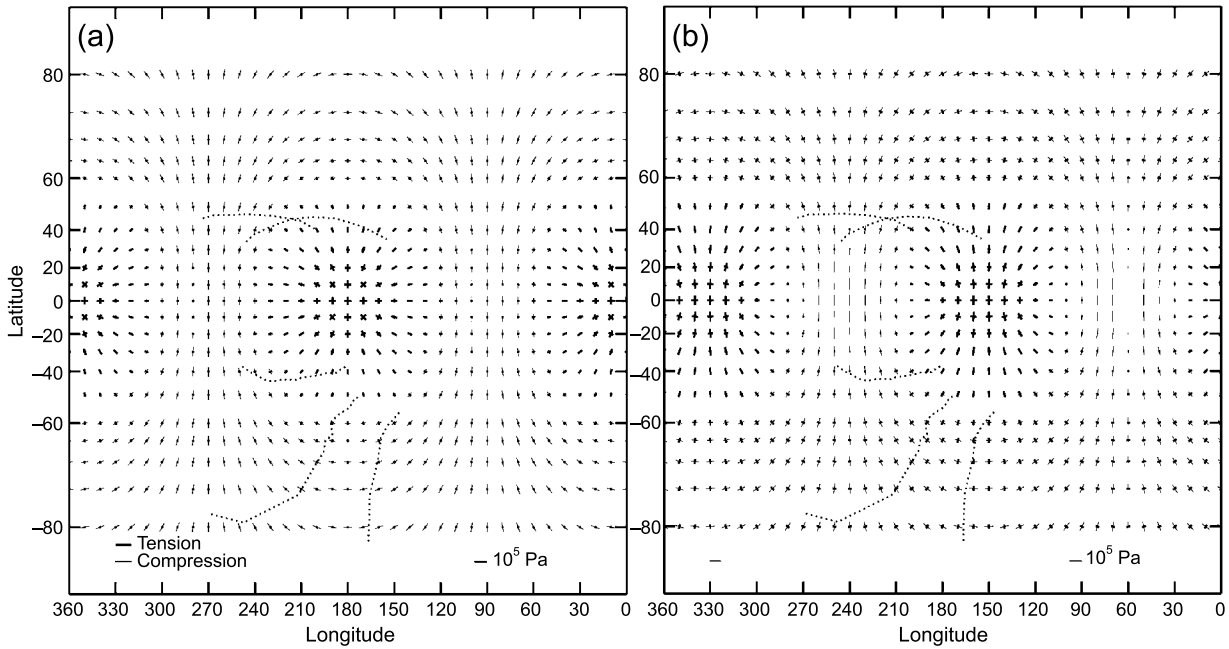

Figure 2. Maps of stress induced due to 'diurnal' variation of the tide, caused by the orbital eccentricity, which in turn is driven by the Laplace resonance with Io and Ganymede. The stress field is shown at intervals of 1/8 of an orbit, starting at pericenter (a). Maps are shown covering only 1/2 of an orbit, because the stress field is anti-symmetrical over time (identical except for a reversal of sign at times 1/2 a period apart). Note that 1/4 of an orbit before or after (c) pericenter, the stress is identical to an equivalent amount of non-synchronous rotation (cf. Figure 1).

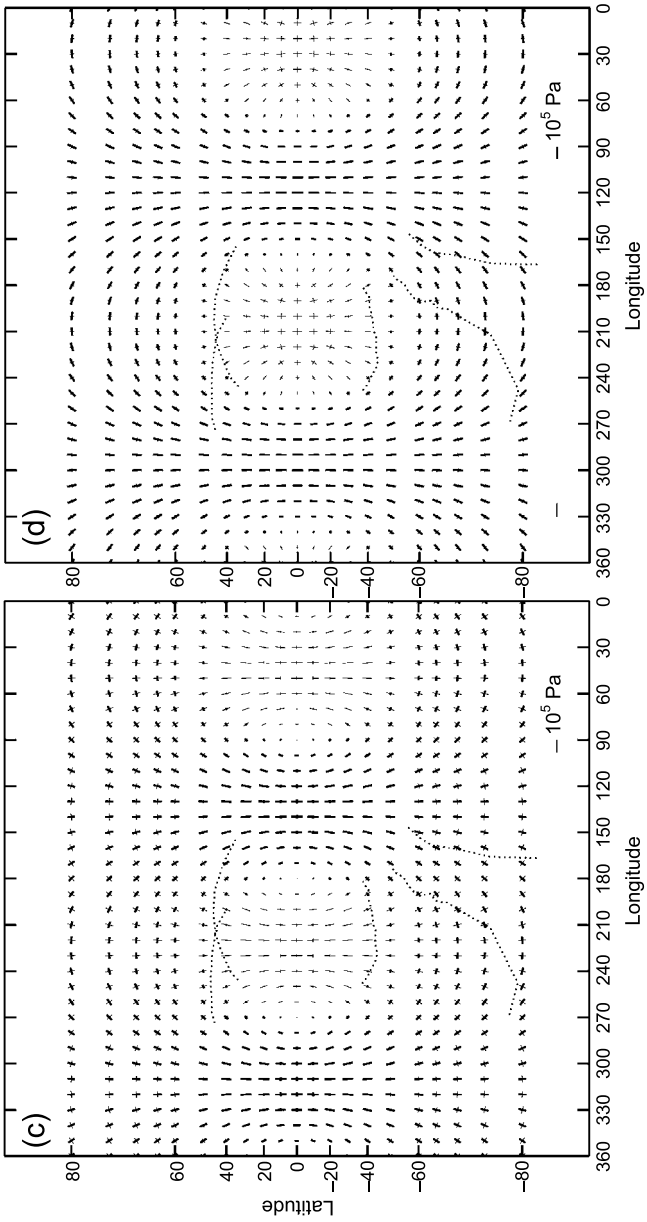

Figure 2. (continued)

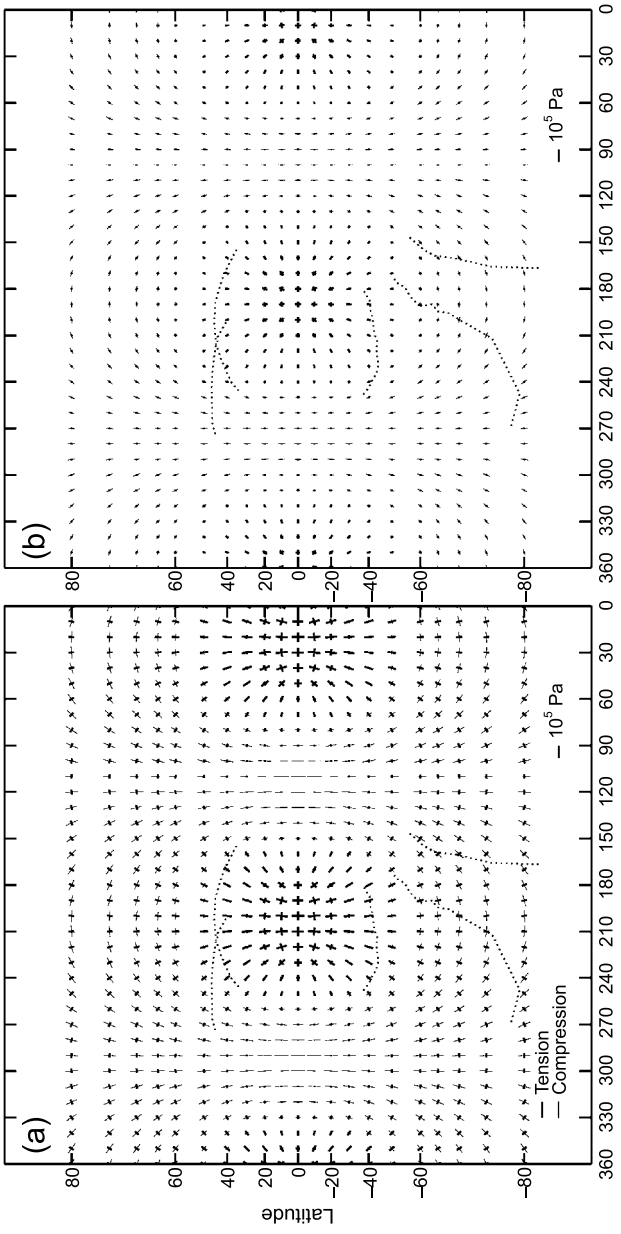

Figure 3. Maps of stress due to 'diurnal' variation of the tide, added to the stress accumulated during 1° of non-synchronous rotation. The stress field is shown at intervals of 1/8 of an orbit, starting at pericenter (a). Maximum tension occurs approximately 1/8 of an orbit after apocenter (f).

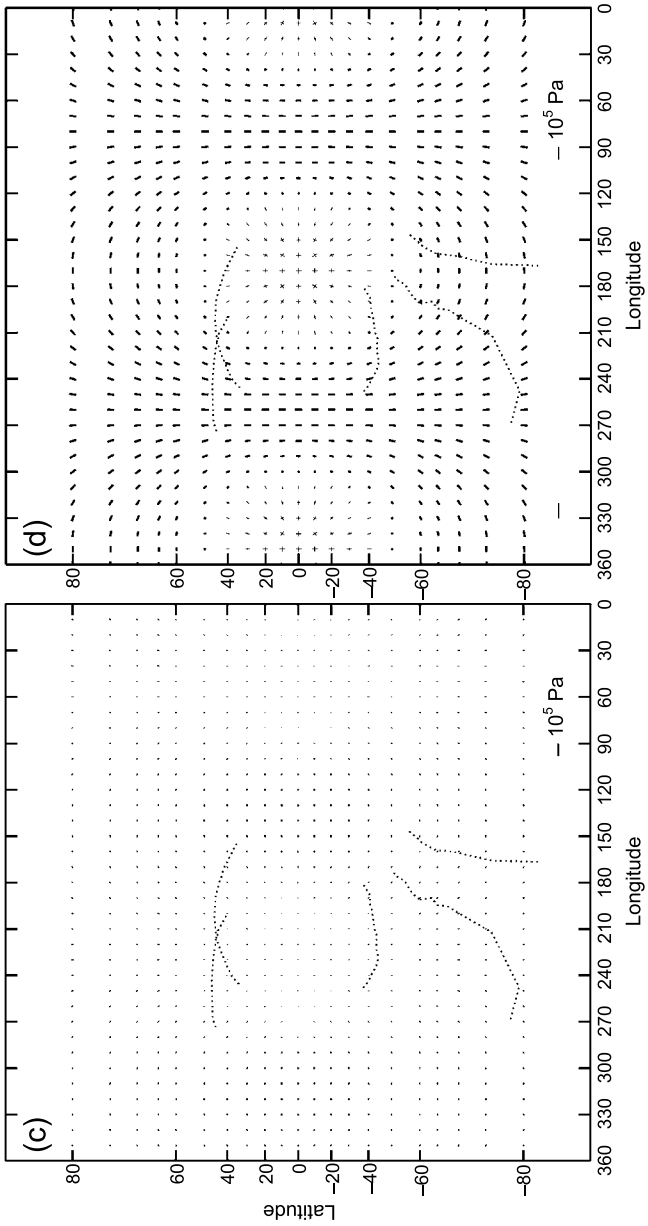

Figure 3. (continued)

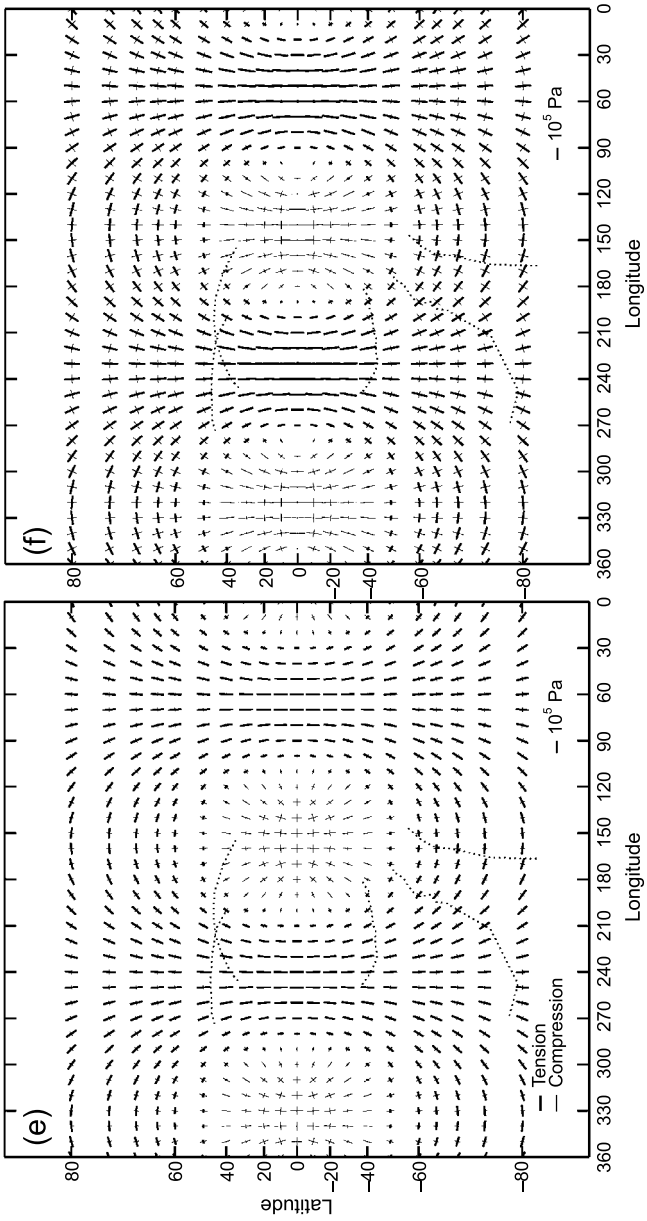

Figure 3. (continued)

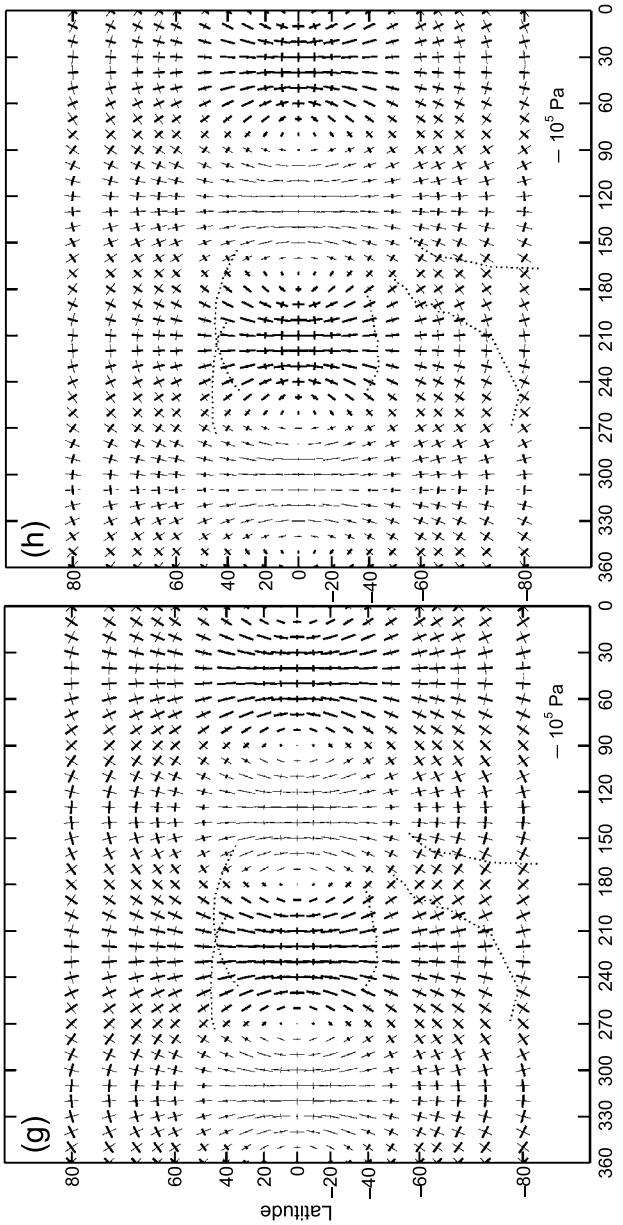

Figure 3. (continued)

Schubert, 1982). A better estimate for the rigidity of ice may be $\mu = 3.52 \times 10^9$ (Gammon et al., 1983), but of course the global effective rigidity of the shell is uncertain. Because the amplitude of the stress is proportional to μ, the stress plots shown here can be applied to any assumed rigidity by simply adjusting the stress scale accordingly.

Figure 1 shows the surface stress field that would accumulate as non-synchronous rotation reoriented the bulge by an angle of 1°, starting with the sub-Jupiter point at 0° longitude. This Mercator projection shows principal axes of stress in their true azimuth orientations. Note that there is pure shear at the poles, where the principal stresses are equal in magnitude but one is tension and the other is compression. Along the equator, in the quadrants moving eastward towards the maximum tidal bulge, there is tension, while in the quadrants moving away from the bulges, there is compression.

For any very small angle of rotation, the pattern is similar, with amplitudes approximately proportional to the angle, and with symmetry offset from the cardinal longitudes (0°, 90°, 180°, 270°) by 45°. For example the tension zones are centered at 45° west of the sub- and anti-Jupiter longitudes, similar to Figure 1. More precisely, however, the pattern is actually shifted eastward from that orientation by a distance equal to half the rotation angle. Thus, if strain could accumulate over rotation by 30° (an example that would be possible only if the material were sufficiently elastic and strong), the stress patterns would be similar except oriented eastward by 15°, such that maximum tension would be 30° west of the sub- and anti-Jupiter longitudes. (The displacement of the pattern by half of the rotation angle is a familiar consequence of taking the difference between sinusoidal functions offset in phase.)

The stress patterns shown in Figure 1 can also be applied to a case of polar wander, if and only if the shift is about an axis aligned with the direction of Jupiter. Suppose the ice shell slips as a whole, so that a location on the ice formerly near the pole moves toward the equator along a meridian 90° from Jupiter. There is evidence for at least one such event in the recent history of Europa (Sarid et al., 2002), and likely there have been many more. In such a case, the stress pattern due to reorientation relative to the equatorial bulge would be the same as non-synchronous rotation relative to the tidal elongation, except that now the bulge is replaced by flattening (changing the sign of the stress at each location) and the reorientation is about an axis lying on the equator, thus shifting the entire stress patterns by 90° relative to Figure 1. As long as appropriate care is taken for those geometric corrections, the pattern shown in Figure 1 could thus be applied to polar wander.

The magnitude of the tension for 1° of non-synchronous rotation is comparable to the plausible tensile strength of the ice, and tension is the most likely mode of failure. Even at high latitudes, where there is a substantial differential between principal stresses, the failure mode would not be shear (contrary to the results of Helfenstein and Parmentier, 1985), because the principal stresses are nearly equal

and opposite; if failure occurred, it would be tensile, according to consideration of the relationship between Mohr's circle and the failure envelope (Suppe, 1985). Figure 1 includes the locations of several major large-scale lineaments of interest, confirming that they are orthogonal to the direction of tension, consistent with that cracking process. Because tension exceeds the strength of the material for more than about 1° of rotation, it is unlikely that more rotation can occur before stress is relieved by cracking. Depending on the rate of rotation, below the surface stress could also be prevented from building up by viscous relaxation of the ice.

3. Stress due to Diurnal Tides

While the non-synchronous rotation period is very long, Europa's orbital period is only about 3.6 days. Periodic tidal variations due to the orbital eccentricity operate on this much shorter timescale. We call these tides 'diurnal' because the orbital period is close to the length of a day on Europa, and of the same order as a terrestrial day, but they are really locked to the orbital period.

With an eccentric orbit, even with synchronous rotation, the magnitude and orientation of the tidal distortion changes throughout each orbital period. The tide-raising gravitational potential is at a maximum at pericenter and a minimum at apocenter. Moreover, the orientation of the tide advances ahead relative to the body of the satellite after pericenter and falls behind before pericenter due to the keplerian variations in orbital angular velocity.

The height of the diurnal tidal variation is $3e$ times the value of H from Equation (1), a result derived from the change in H due to replacing the distance from Jupiter a with the pericenter distance $a(1 - e)$ or apocenter distance $a(1 + e)$. Thus for Europa with $e = 0.01$, the amplitude is 30 m, that is, the tidal height at the sub- and anti-Jove points at pericenter (or apocenter) is 30 m higher (or lower) than the surface of the fixed tide given by Equation (1). Between apocenter and pericenter, specifically 1/4 orbit before and after pericenter, Europa is at the mean distance from Jupiter, so the tidal figure is given by Equation (1), except that the orientation of the tidal elongation is rotated by an angle $\pm 2e$ (about 1.5°). The change in orientation of the elongation of Europa between these states does not represent rotation of the body, but rather a 'remolding' of the figure of Europa in response to the changing direction of Jupiter.

We have computed the tidal stress at various points in the orbit as shown in Figure 2(a–d) relative to the average figure of Europa. By average figure, we mean the tidal shape that would represent the response to Jupiter if there were no orbital eccentricity, that is, if Jupiter were at the center of its orbital epicycle relative to Europa.

At pericenter (Figure 2(a)), the stress patterns are exactly the same as those generated by distorting a spherical shell into a tidally elongated shape, because only the amplitude differs from the average configuration. Here with the distance

from Jupiter at a minimum, the amplitude of the tidal bulge is a maximum, giving isotropic tension at the sub- and anti-Jupiter points and compression along the belt 90° from those points. Figure 2 also shows the stress 1/8 orbit after pericenter (Figure 2(b)), 1/4 orbit after pericenter (Figure 2(c)), and 3/8 orbit after pericenter (Figure 2(d)). The stress map at pericenter (or at any orbital position 1/2 orbit from the positions shown) would be identical to the cases shown in Figure 2, except that the signs of the principal components are reversed (tension becomes compression and vice versa).

Because ice is most prone to failure in tension, we are especially interested in locations and conditions of maximum tension. The stress pattern at apocenter (Figure 2(a) with signs reversed), like the pattern due to non-synchronous rotation (Figure 1), has equatorial regions of north–south tension, although centered at quite different longitudes. Moreover, the tension extends across the poles, contrasting with the non-synchronous case where tension near the poles is accompanied by comparable orthogonal compression yielding shear stress. In both cases (Figure 1 and diurnal stress at pericenter) the vectors of maximum tension form ellipses encircling regions that are under compression on the equator: at 0° and 180° for the diurnal stress; at 135° and 315° for non-synchronous stress.

It is important to remember that the diurnal tide is not simply due to the changing distance from Jupiter, but also to the changing direction of Jupiter. At 1/4 orbit before or after pericenter, the tidal amplitude is identical to the average, but the orientation is shifted by about 1.5°, equivalent to non-synchronous rotation (compare Figure 2(c) with Figure 1, noting that the stress pattern is practically identical, except for the difference in sign and that the magnitude is 50% larger, in proportion to the angular offset of the tidal bulge).

On Europa, tidal stress results from a combination of diurnal and non-synchronous effects. Figure 3 shows the combined stress of 1° of non-synchronous and diurnal stress over an entire orbit. Greenberg et al. (1998) suggested that diurnal stress alone might not be sufficient to explain cracking or the crack patterns observed. Instead, a background stress builds up as the tidal bulge gradually migrates due to non-synchronous rotation. That background stress field is superimposed on the diurnally varying component of the tidal stress, until one day the maximum tensile stress exceeds the strength of the ice. According to Figure 3, that event probably occurs about 1/8 of an orbit after apocenter. As described by Greenberg et al. (1998), this model seems most consistent with the systematic variation in crack orientations noted in the northern trailing hemisphere by Geissler et al. (1998a, b).

4. Stress Change During Crack Propagation

The stress patterns shown in any of the stress diagrams (Figures 1–3) can be converted to predictions of crack orientations that might result. For example, at

a given location, tensile cracks would be perpendicular to the maximum principal component in tension. However, the ubiquitous cycloidal crack features on Europa (arcs about 100 km long, connected at cusps, and extending in chains typically 1,000 km or more long) do not match the stress field at any given time. Instead, as shown by Hoppa et al. (1999b), they can be explained by taking into account the finite rate of propagation of a given crack, such that the orientation of the dominant stress at the propagation tip is continuously varying with time as well as place. A crack propagates along a curve as the time-variation causes a change in the orientation of the tensile stress, then it stops when the magnitude of the stress decreases below a critical value, restarting later along a new arc when the stress has increased sufficiently.

Figure 4 shows the global distribution of crack patterns predicted to form due to diurnal stress variations according to the theory of Hoppa et al. (1999b). Here we have simulated the propagation from starting points spaced evenly in 10° intervals in latitude and longitude, with propagation starting toward the west. (Similar patterns are produced for eastward propagation.) The crack patterns depend on the rate of crack propagation, which controls the curvature of each arc, and on the stress levels required to start and to maintain crack propagation, which determine the start and stop points for each arc forming cusps. These theoretical crack patterns depend on the parameters assumed to characterize the ice. In Figure 4, we assume a rigidity $\mu = 3.52 \times 10^9$, crack propagation speed of 7 km/h, a strength of 0.19 bar for crack initiation, and a limit of 0.13 bar, below which propagation ceases. These

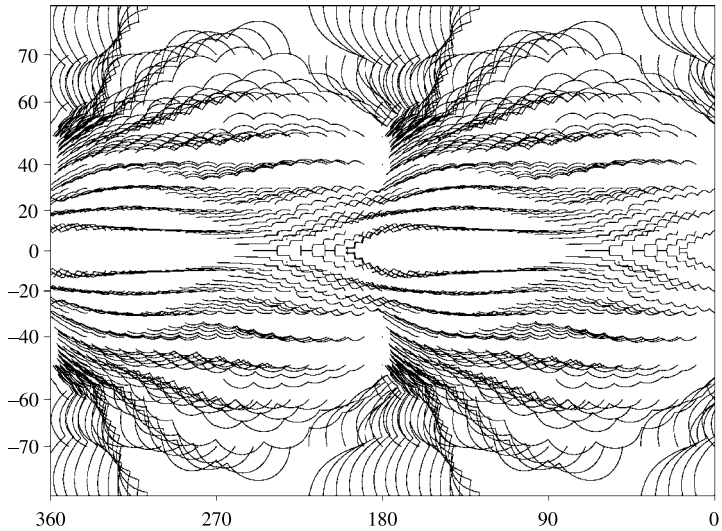

Figure 4. Theoretical patterns produced as cracks propagate at a finite speed (7 km/h) through a diurnally changing stress field from starting points spaced every 10° in latitude and longitude and propagating initially westward. The general shape is cycloidal, although rounded boxy patterns are produced as well, in good agreement with observed crack patterns (Figure 5).

Figure 5. A preliminary map of observed cycloidal lineaments on Europa, marked in black. The features are indicated on a background mosaic image in a Mercator projection. The map includes the extreme cases that form circular-to-boxy patterns, which are found in the 'wedges' region south of the equator around 200° longitude and diametrically opposite in the sub-Jovian hemisphere. These features lie near where stress patterns suggest that cracks of this shape and size should form (Figure 4).

parameters are plausible for Europan ice, and they yield cycloids similar to those observed on Europa.

For comparison, Figure 5 shows a map of cycloidal lineaments actually observed on Europa. (This map is affected by observational selection: The clustering in certain regions is due to the fact that imaging conditions were not uniform.) Several similarities between the theoretical distribution and the observed features are of note. First, at latitudes of $-50°$ to $-60°$, the shapes and scale of the theoretical cycloids are similar to the classical examples observed at those latitudes in Voyager images, although the locations are not in agreement, probably because rotation has shifted the positions since the cycloidal cracks were formed (Hoppa et al., 2001; Greenberg et al., 2002b).

A second similarity is the tendency for long, east–west chains just north and south of the equator, which are quite prominent on the theoretical plot (Figure 4). These are observed on Europa (Figure 5) at those latitudes, especially in the sub- and anti-Jovian regions (around 0° and 180° longitude). They cannot be seen at other longitudes, either because image resolution is inadequate, or because such tectonic features have been disrupted by the formation of extensive chaotic terrain (as from 240° to 340° longitude).

Cycloids that run north–south on Europa (Figure 5) tend to be relatively short, and are usually far from the equator. This observation is also consistent with the patterns predicted by the tidal-stress theory (cf. Figure 4).

Finally, we note that the surface of Europa displays boxy or circular crack patterns in the anti-Jovian hemisphere just south of the equator in a region called the 'wedges region' (named for the wedge-shaped dilational openings that are common along cracks there. Similar, but more subtle crack patterns also appear on the sub-Jovian hemisphere. These observed crack features (marked in Figure 5) in both the wedges region and 180° away in the sub-Jovian region lie at the theoretically predicted locations for such boxy crack shapes (shown in Figure 4). The similarity in shape and scale of the observed features to those predicted is striking.

If the theoretical parameters were substantially different from those used here, the shapes of the predicted crack patterns would be very different (Bart et al., 2002). Given uncertainty about the character of the actual material on Europa, the appropriate *a priori* parameter choices are poorly constrained. However, we find that the parameters used here yield remarkable agreement with various observed tectonic patterns on a global scale. The same parameter choices that allowed Hoppa et al. (2001) to fit the shapes of the cycloids in Voyager images also fit other crack patterns on Europa, as discussed above, suggesting that they do represent reasonably well the material properties of Europa's crust, and that they are remarkably uniform.

These results represent only a preliminary study. A more comprehensive comparison of theoretical crack patterns and what is observed on Europa is under way. The objective is to understand the origins of the observed crack patterns and to exploit them as a means to reconstruct the history of rotation and polar wander. Such work has already been pioneered (e.g. by Geissler et al., 1998a, b; Hoppa et al., 2001; Sarid et al., 2002), but the available image data set allows the possibility of extending these approaches further in time and in detail.

5. Conclusion

Europa has been actively resurfaced recently compared with the age of the solar system, and these processes may be on-going (Greenberg et al., 2002a). Tides have driven this resurfacing by both heat and stress. The tectonic record can be compared with theoretical models of tidal stress. This approach has helped explain the general patterns of global lineaments, regional time sequences of crack orientations, strike-slip displacement, and cycloidal crack patterns. Continuing research is extending that work to explain observed tectonics in more detail, and to understand long-term evolution. Comparison of tidal theory with the time-sequences of formation of tectonic features, from geological cross-cutting relationships for example, is allowing us to place constraints on the rotational history. The maps of theoretical tidal stress patterns presented here may help support continuing progress toward reconstruction of the history of Europa's rotation and polar wander. They may also prove useful for considering stress on any other bodies, such as Io or the satellites

of Saturn, where an observable geological record might be correlated with tidal stress.

Acknowledgements

We thank Iwan Williams, Yuehua Ma, and the other organizers for inviting the presentation and arranging the colloquium, and Sylvio Ferraz-Mello for coordinating publication of papers from the conference. This research is supported by a grant from NASA's Planetary Geology and Geophysics program.

References

Anderson, J. D. et al.: 1998, 'Europa's differentiated internal structure: Inferences from four Galileo encounters', *Science* **281**, 2019–2022.

Bart, G. D., Greenberg, R., Hoppa, G. V. and Hurford, T. A.: 2002, 'Global patterns of diurnal tensile cracking on Europa', *Bull. Amer. Astron. Soc.* **34**, 915.

Figueredo, P. H. and Greeley, R.: 2000, 'Geologic mapping of the northern leading hemisphere of Europa', *J. Geophys. Res.* **105**, 22629–22646.

Gammon, P. H., Klefte, H. and Klouter, M. J.: 1983, 'Elastic constants of ice samples by Brillouin spectroscopy', *J. Phys. Chem.* **87**, 4025–4029.

Geissler, P. et al.: 1998a, 'Evidence for non-synchronous rotation of Europa', *Nature* **391**, 368–370.

Geissler, P. et al.: 1998b, 'Evolution of lineaments on Europa: Clues from Galileo multispectral imaging observations', *Icarus* **135**, 107–126.

Greenberg, R.: 1982, 'Orbital evolution of the galilean satellites'. In: D. Morrison (eds), *The Satellites of Jupiter*, University of Arizona Press, Tucson, pp. 65–92.

Greenberg, R.: 1989, 'Time-varying orbits and tidal heating of the galilean satellites', In: Belton, M. J. S., West, R. A. and Rahe, J. (eds), *Time-Variable Phenomena in the Jovian System*, NASA Special Publication No. 494.

Greenberg, R.: 2002, 'Tidal processes and the geophysics of Europa (invited review)', In: *IAU Colloquium No. 189 "Astrophysical Tides"*, Nanjing, China.

Greenberg, R. and Weidenschilling, S. J.: 1984, 'How fast do Galilean satellites spin?', *Icarus* **58**, 186–196.

Greenberg, R. et al.: 1998, 'Tectonic processes on Europa: Tidal stresses, mechanical response, and visible features', *Icarus* **135**, 64–78.

Greenberg, R. et al.: 2002a, 'Tidal tectonic processes and their implications for the character of Europa's icy crust (invited review)', *Rev. Geophysics* **40**(2), 1004.

Greenberg, R., Hoppa, G. V., Geissler, P., Sarid, A. and Tufts, B. R.: 2002b, 'The rotation of Europa', *Celestial Mechanics and Dynamical Astronomy* **83**, 35–47.

Helfenstein, P. and Parmentier, E. M.: 1983, 'Patterns of fracture and tidal stresses on Europa', *Icarus* **53**, 415–430.

Helfenstein, P. and Parmentier, E. M.: 1985, 'Patterns of fracture and tidal stresses due to nonsynchronous rotation: Implications for fracturing on Europa', *Icarus* **61**, 175–184.

Hoppa, G. V. et al.: 1999a, 'Strike-slip faults on Europa: Global shear patterns driven by tidal stress', *Icarus* **141**, 287–298.

Hoppa, G. V. et al.: 1999b, 'Formation of cycloidal features on Europa', *Science* **285**, 1899–1902.

Hoppa, G. V. et al.: 2000, 'Distribution of strike-slip faults on Europa', *J. Geophys. Res.-Planets* **105**, E9, 22617–22627.

Hoppa, G. V. et al.: 2001, 'Europa's rate of rotation derived from the tectonic sequence in the Astypalaea region', *Icarus* **153**, 208–213.

Kattenhorn, S. A.: 2002, 'Nonsynchronous rotation evidence and fracture history in the Bright Plains region, Europa', *Icarus* **157**, 490–506.

McEwen, A. S.: 1986, 'Tidal reorientation and the fracturing of Jupiter's moon Europa', *Nature* **321**, 49–51.

Melosh, H. J.: 1980, 'Tectonics patterns on a tidally distorted planet', *Icarus* **43**, 334–337.

Moore, W. B. and Schubert, G.: 2000, 'The tidal response of Europa', *Icarus* **147**, 317–319.

O'Brien, D. P., Geissler, P. and Greenberg, R.: 2002, 'A melt-through model for chaos formation on Europa', *Icarus* **156**, 152–161.

Peale, S. J. and Lee, M. H.: 2002, 'A primordial origin of the Laplace relation among the Galilean satellites', *Science* **298**, 593–597.

Sarid, A. R., Greenberg, R., Hoppa, G. V., Hurford, T. A., Tufts, B. R. and Geissler, P.: 2002, 'Polar wander and surface convergence on Europa: Evidence from a survey of strike-slip displacement', *Icarus* **158**, 24–41.

Suppe, J.: 1985, *Principles of Structural Geology*, Prentice-Hall, Englewood Cliffs, NJ.

Turcotte, D. L. and Schubert, G.: 1982, *Geodynamics*, Wiley, New York.

Vening-Meinisz, F. A.: 1947, 'Shear patterns of the Earth's crust', *Trans. AGU* **28**, 1–61.

Yoder, C. F. and Sjogren, W. L.: 1996, 'Tides on Europa', In: *Europa Ocean Conference*, San Juan Capistrano Institute, San Juan Capistrano, California, p. 89.

Zahnle, K. et al.: 1998, 'Cratering rates on the Galilean satellites', *Icarus* **136**, 202–222.